Crystal Packing of Two Different Tetranuclear Iron(III) Clusters, $[(tacn)_4Fe_4O_2(OH)_4]_2 \cdot 8Br \cdot 9H_2O$ (tacn = 1,4,7-triazacyclononane)

Mi Kyung Jin, YooJin Kim, Duk-Young Jung,* Min Heu,† Seokwon Yoon,‡ and Byoung Jin Suh‡

Department of Chemistry-BK21 and the Institute of Basic Sciences, Sungkyunkwan University, Suwon 440-746, Korea
**E-mail: dyjung@skku.edu*
†Department of Physics, The Catholic University of Korea, Bucheon 420-743, Korea
Received September 3, 2004

$[(tacn)_4Fe_4O_2(OH)_4]_2 \cdot 8Br \cdot 9H_2O$ (tacn = 1,4,7-triazacyclononane), a tetranuclear iron(III) complex was synthesized by the hydrolysis of $(tacn)FeCl_3$ and crystallizes in the orthorhombic space group, *Pca2(1)*, with cell parameters, a = 37.574(3) Å, b = 16.9245(12) Å, c = 14.2830(11) Å, V = 9082.9(12) Å^3. $[(tacn)_4Fe_4O_2(OH)_4]^{4+}$ cations approach S_4 point symmetry containing an adamantane skeleton. Four Fe(III) atoms have distorted octahedral environments with two hydroxo and an oxo bridges. Two $[(tacn)_4Fe_4O_2(OH)_4]^{4+}$ clusters having different Fe···Fe distances are connected to each other by the networked hydrogen bonds. The electrochemical behavior reveals irreversible three cathodic and two anodic peaks. Magnetic properties are characterized by antiferromagnetic (AF) interactions between Fe(III) ion spins. However, the low-lying states are still magnetic and exhibit a blocking behavior and a magnetic hysteresis at low temperatures.

Key Words : Iron(III), Tetranuclear complex, Tacn, Magnetic properties

Introduction

The polynuclear hydroxo- and oxo-bridged metal complexes are full of interest from diverse viewpoints, containing the field of molecular based magnets, structural and functional biomimic models for active sites of some metalloproteins.[1-3] Hemerythrin, ribonucleotide reductase, methane monooxygenase, and purple acid phosphatase contain binuclear iron centers,[4] and ferritins and hemosiderins consist of iron cluster units of uncertain size.[5] The polynuclear metal complexes have a wealth of interesting topologies, including ferric wheels,[6] can also function as nanoscale magnets called `single molecule-magnets (SMMs)`.[7] The SMMs show quantum tunneling of magnetization in the hysteresis loops as a bridge linking classical to quantum magnetic behavior. Several examples of SMMs have been reported, which contain iron (Fe_8[8] and Fe_4[9]) and manganese (Mn_{12}[10] and Mn_4[11]) ions. One of the most intensively investigated SMMs is an octanuclear iron complex, commonly called "Fe_8", $[(tacn)_6Fe_8O_2(OH)_{12}]Br_8$ (tacn=1,4,7-triazacyclononane).[12] The tacn ligand, cyclic tridentate amine ligand is facially coordinated to the octanuclear iron complex and each iron ion of Fe_8 coupled together by twelve hydroxo and oxo bridges. The Fe_8 compound is prepared by the controlled hydrolysis of $(tacn)FeCl_3$ and by chance, we discovered that a tetranuclear iron cluster was obtained in the similar conditions. The tetranuclear iron clusters show several types of structure, including the adamantane, butterfly, tetragon, planar and face-to-face types.[13] The tetranuclear iron complex in this work reveals an adamantane shape with facially coordinated tacn ligands, and this compound is shown to be composed of a racemic mixture. Unusually, two tetranuclear iron complexes showing the similar adamantane skeletons but the different Fe···Fe distances were found in the crystal structure of the prepared Fe_4 compound.

Herein, we present the synthesis, structural analysis by single-crystal X-ray diffraction, electrochemical and magnetic characterization of the adamantane-like tetranuclear iron cluster of formula $[(tacn)_4Fe_4O_2(OH)_4]_2 \cdot 8Br \cdot 9H_2O$ (where tacn = 1,4,7-triazacylononane).

Experimental Section

Synthesis of $\{[(tacn)_4Fe_4O_2(OH)_4]\}_2 \cdot 8Br \cdot 9H_2O$. $(tacn)FeCl_3$ used as a precursor was prepared based on literature procedures.[14] NaBr (6.00 g, 58.31 mmol) was added to a yellow aqueous solution (16 mL) of $(tacn)FeCl_3$ (0.44 g, 1.51 mmol) with stirring. This orange color solution adjusts to pH 10.28 and stood at 25 °C. The black octahedral shaped crystals were obtained within one day and collected by filtration; yield ~26.3% based on total $(tacn)FeCl_3$.

Anal. (wt%). Calcd for $[(tacn)_4Fe_4O_2(OH)_4] \cdot 4Br \cdot 4.5H_2O$: Fe, 18.00; C, 23.21; H, 5.88; N, 13.5; O, 13.54. Found: Fe, 17.75; C, 23.33; H, 5.89; N, 13.77; O, 13.33. IR (KBr pellet, cm^{-1}, selected peaks): 3421(br), 3211(br), 2970(s), 2918(s), 2864(s), 1637(s), 1448(s), 1359(s), 1105(m), 1024(s), 926(m), 868(s), 769(m).

Crystal Structure Determination. A black crystal with dimensions 0.40 × 0.20 × 0.20 mm^3 was glued to a glass fiber and mounted on the goniometer. Preliminary examination and data collection were performed with Mo-Kα radiation (λ = 0.71069 Å) on a Siemens SMART CCD equipped with a graphite crystal, incident-beam monochromator. Data were collected at 173 K. Cell parameters were determined and refined using the SMART software, raw frame data were integrated using the SAINT programs, which corrects for Lorentz and polarization effects.[15]

Table 1. Crystallographic Data for $[(tacn)_4Fe_4O_2(OH)_4]_2 \cdot 8Br \cdot 9H_2O$

Empirical formula	$C_{48}H_{146}Br_8Fe_8N_{24}O_{21}$
Formula weight	2482.02
Temperature	173(2) K
Wavelength	0.71073 Å
Crystal system	Orthorhombic
Space group	*Pca2(1)*
a, Å	37.574(3)
b, Å	16.9245(12)
c, Å	14.2830(11)
Volume, Å^3	9082.9(12)
Z	4
Density (calculated)	1.796 Mg/m^3
θ range for data collection	1.08 to 28.35°
Reflections collected	55530
Independent reflections	16035 [R(int) = 0.0502]
Data / restraints / parameters	16035 / 1 / 1079
Goodness-of-fit on F^2	1.012
Final R indices [$I > 2\sigma(I)$]	$R = 0.0470$, $R_w = 0.1023$
R indices (all data)	$R = 0.0751$, $R_w = 0.1153$

Empirical absorption correction was applied with the program SADABS.[16] The pattern of systematic absences observed in the data was consistent with either the space group *Pca2(1)* which was assumed and confirmed by the successful solution and refinement of the structure.

A summary of crystal data is represented in Table 1. The structure was solved by direct methods (SHELX-86) and standard difference Fourier techniques (SHELX-97).[17] All non-hydrogen atoms were refined anisotropically; all hydrogen atoms attached to carbon, nitrogen and oxygen atoms were added theoretically according to electron density difference. Refinements were performed by full-matrix least-squares analysis, with anisotropic thermal parameters for all non-hydrogen atoms and with isotropic ones for all hydrogen atoms. The reliability factors converged to R (F_o) – 0.0470 and *Rw* (F_o^2) – 0.1023.

Characterizations. Electrochemical experiments were performed with a Princeton Applied Research (PAR) Model 263A potentiostat. Electrochemical measurements were made on methylene chloride solutions containing 0.1 M tetra-n-butylammonium hexafluorophosphate ($TBAPF_6$) as supporting electrolyte and were conducted at room temperature. A standard three-electrode system was used for cyclic voltammetry (CV) and differential potential voltammetry (DPV) experiments comprising a platinum working electrode, a platinum auxiliary electrode, and an Ag/AgCl (saturated KCl solution) electrode.

Infrared spectroscopy using a dry KBr pellet was performed on a Nicolet FT-IR 1700 spectrophotometer in the range of 4000-400 cm^{-1}. Electronic absorption in 200-700 nm range was collected using an Optizen III UV/vis spectrophotometer at room temperature.

Magnetization was measured for ground single crystals using a conventional SQUID magnetometer (Quantum Design MPMS-XL7) as functions of temperature and field.

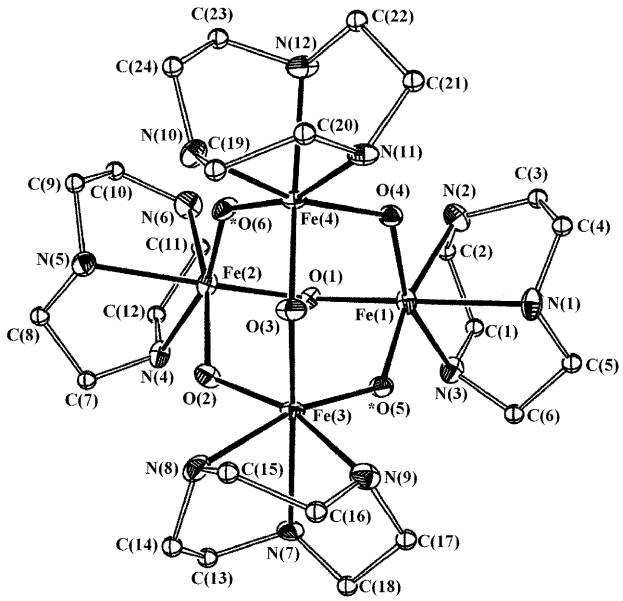

Figure 1. Structure of $[(tacn)_4Fe_4O_2(OH)_4]_2 \cdot 8Br \cdot 9H_2O$ showing 40% probability ellipsoids and atom labeling scheme. *O designates oxo oxygen atom. For clarity, hydrogen atoms are omitted.

All the data were corrected for the diamagnetic background of the sample holder.

Results and Discussion

Crystal Structure. Fe and O atoms in the $[(tacn)_4Fe_4O_2(OH)_4]^{4+}$ cation (hereafter Fe4) present the adamantane shape[18-22] with Fe atoms occupying the vertexes of a tetrahedron and O atoms those of an octahedron as shown in Figure 1. Each Fe(III) atom is coordinated to three oxygen atoms from an oxo and two hydroxo ligands and three nitrogen atoms from the facially coordinated tacn ligand in a distorted octahedral environment. The four hydroxo, O(1), O(2), O(3) and O(4) in Figure 1, lie in the plane perpendicular to the axis passing through two oxo ligands, O(5) and O(6). The average Fe···Fe distance is 3.462 Å, close to 3.465 Å, the value of observed for $[(tacn)_4Fe_4O_2(OH)_4]I_4 \cdot 3H_2O$ [19] and 3.45 Å for Fe8, which arises from the corner-sharing octahedra via oxo- or hydroxo-bridges.[12]

In Table 2, the selected bond and angles are summarized. In the Fe4 cluster, there are two groups of Fe–O bond lengths and Fe–O–Fe angles since each Fe atom is coordinated to both hydroxo and oxo oxygens. In Figure 2, O(2) oxygen atom comes from hydroxo and O(5) oxygen atom from oxo ligand, respectively. Four hydroxo bridges are characterized by an average Fe–O(hydroxo) bond length of 1.982(6) Å, ranging between 1.939 and 2.033 Å and an average Fe–O(hydroxo)–Fe angle of 124.9(3)° (123.1-126.6°). The remaining two oxo bridges consist of shorter Fe–O(oxo) bonds of 1.837(5) Å in the range of 1.832-1.844 Å and larger Fe–O(oxo)–Fe angles of 132.3(3)° in the range of 131.4-133.1°.[19,20] In general, the stronger donor atoms would be expected to have the shorter metal-ligand bond lengths. The crystallographic data of Fe4 coincide with this

Table 2. Selected Bond Distances (Å) and angles (°) for $[(tacn)_4Fe_4O_2(OH)_4]2{\cdot}8Br{\cdot}9H_2O$

	bond distances		
Fe(1)···Fe(3)	3.353(1)	Fe(2)···Fe(4)	3.366(1)
Fe(1)···Fe(4)	3.477(4)	Fe(2)···Fe(1)	3.533(2)
Fe(2)···Fe(3)	3.510(1)	Fe(3)···Fe(4)	3.537(5)
Fe(1)–O(5)	1.836(5)	Fe(3)–O(5)	1.844(5)
Fe(1)–O(4)	1.975(6)	Fe(3)–O(2)	1.961(6)
Fe(1) O(1)	2.010(5)	Fe(3) O(3)	2.033(7)
Fe(1)–N(1)	2.203(6)	Fe(3)–N(7)	2.177(7)
Fe(1)–N(3)	2.208(7)	Fe(3)–N(9)	2.237(6)
Fe(1)–N(2)	2.240(7)	Fe(3)–N(8)	2.249(7)
Fe(2) O(6)	1.837(6)	Fe(4) O(6)	1.832(5)
Fe(2)–O(2)	1.968(6)	Fe(4)–O(4)	1.939(6)
Fe(2)–O(1)	1.982(5)	Fe(4)–O(3)	1.990(6)
Fe(2)–N(6)	2.200(6)	Fe(4)–N(10)	2.210(7)
Fe(2) N(5)	2.212(6)	Fe(4) N(12)	2.223(7)
Fe(2)–N(4)	2.241(7)	Fe(4)–N(11)	2.246(6)
Fe(5)···Fe(7)	3.555(1)	Fe(6)···Fe(8)	3.521(1)
Fe(5)···Fe(8)	3.541(2)	Fe(6)···Fe(5)	3.314(2)
Fe(6)···Fe(7)	3.550(1)	Fe(7)···Fe(8)	3.294(3)
Fe(5)–O(7)	1.805(5)	Fe(7)–O(9)	1.813(5)
Fe(5)–O(11)	1.997(5)	Fe(7)–O(8)	1.992(6)
Fe(5) O(10)	2.003(5)	Fe(7) O(11)	2.021(5)
Fe(5)–N(14)	2.186(6)	Fe(7)–N(20)	2.183(6)
Fe(5)–N(13)	2.234(7)	Fe(7)–N(19)	2.215(7)
Fe(5)–N(15)	2.241(6)	Fe(7)–N(21)	2.240(7)
Fe(6) O(7)	1.815(5)	Fe(8) O(9)	1.792(6)
Fe(6)–O(8)	2.011(6)	Fe(8)–O(10)	2.004(5)
Fe(6)–O(12)	2.017(5)	Fe(8)–O(12)	2.027(5)
Fe(6)–N(17)	2.220(7)	Fe(8)–N(24)	2.186(6)
Fe(6) N(16)	2.222(6)	Fe(8) N(22)	2.217(6)
Fe(6)–N(18)	2.293(6)	Fe(8)–N(23)	2.288(7)
	bond angles		
O(5) Fe(1) O(4)	100.4(3)	O(6) Fe(4) O(4)	98.4(2)
O(5)–Fe(1)–O(1)	96.0(2)	O(6)–Fe(4)–O(3)	103.8(3)
O(4)–Fe(1)–O(1)	101.5(2)	O(4)–Fe(4)–O(3)	96.5(3)
O(6)–Fe(2)–O(2)	99.0(3)	Fe(2)–O(1)–Fe(1)	124.6(3)
O(6) Fe(2) O(1)	100.2(2)	Fe(3) O(2) Fe(2)	126.6(3)
O(2)–Fe(2)–O(1)	95.4(3)	Fe(4)–O(3)–Fe(3)	123.1(3)
O(5)–Fe(3)–O(2)	104.0(3)	Fe(4)–O(4)–Fe(1)	125.2(3)
O(5)–Fe(3)–O(3)	97.9(3)	Fe(1)–O(5)–Fe(3)	131.4(3)
O(2) Fe(3) O(3)	95.0(3)	Fe(4) O(6) Fe(2)	133.1(3)
O(7)–Fe(5)–O(11)	108.0(2)	O(9)–Fe(8)–O(10)	108.1(2)
O(7)–Fe(5)–O(10)	94.8(2)	O(9)–Fe(8)–O(12)	97.1(2)
O(11)–Fe(5)–O(10)	92.4(2)	O(10)–Fe(8)–O(12)	94.7(2)
O(7) Fe(6) O(8)	95.6(3)	Fe(5) O(7) Fe(6)	132.5(3)
O(7)–Fe(6)–O(12)	104.0(2)	Fe(7)–O(8)–Fe(6)	124.9(3)
O(8)–Fe(6)–O(12)	99.0(2)	Fe(8)–O(9)–Fe(7)	132.0(3)
O(9)–Fe(7)–O(8)	103.0(3)	Fe(5)–O(10)–Fe(8)	124.1(3)
O(9) Fe(7) O(11)	95.6(2)	Fe(5) O(11) Fe(7)	124.4(3)
O(8)–Fe(7)–O(11)	96.3(2)	Fe(6)–O(12)–Fe(8)	121.1(3)

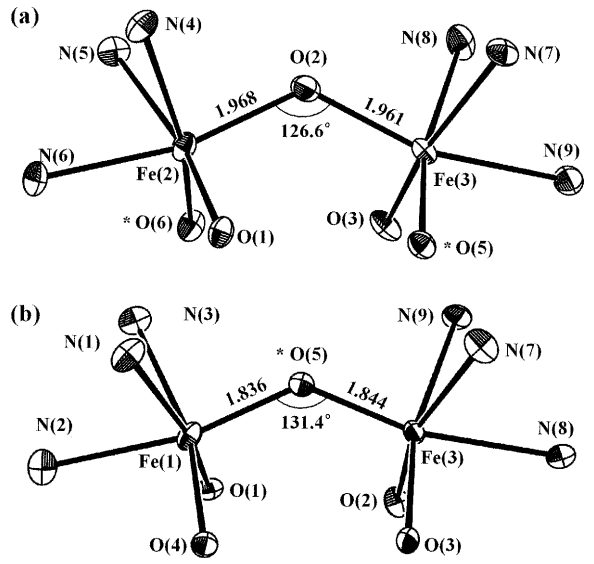

Figure 2. Two Fe–O–Fe types in $[(tacn)_4Fe_4O_2(OH)_4]^{4+}$, long Fe–$O_{hydroxo}$ bonds and small Fe–$O_{hydroxo}$–Fe angles (a), and Fe–O_{oxo} and a Fe–O_{oxo}–Fe ones (b). *O designates oxo oxygen atom. For clarity, carbon atoms from tacn ligands and hydrogen atoms are omitted.

expectation resulting in Fe–O(oxo) bonds slightly shorter than the Fe–O(hydroxo) bonds. Owing to the trans effect, Fe–N bonds (the average value of 2.255(7) Å) trans to oxo ligands are slightly elongated compared with the Fe–N bonds (average of 2.208(7) Å) trans to hydroxo ones. Contrary to the pseudo T_d point symmetry observed for $[(tacn)_4Mn_4O_6]^{4+}$,[21] the Fe4 cation approaches lower symmetry of S_4 with the S_4 axis passing through two oxo ligands resulting from two types of oxygens in the Fe4

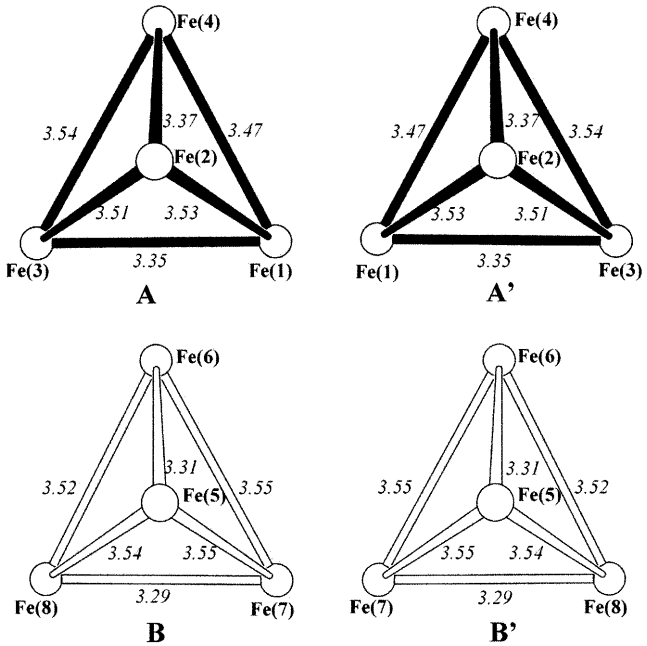

Figure 3. Four kinds of Fe4 cations in the crystal structure of $[(tacn)_4Fe_4O_2(OH)_4]_2{\cdot}8Br{\cdot}9H_2O$. Only Fe···Fe distances are presented, *A* and *B* have different Fe···Fe distances each other. *A'* is an enantiomer of *A* and *B'* is of *B*, respectively.

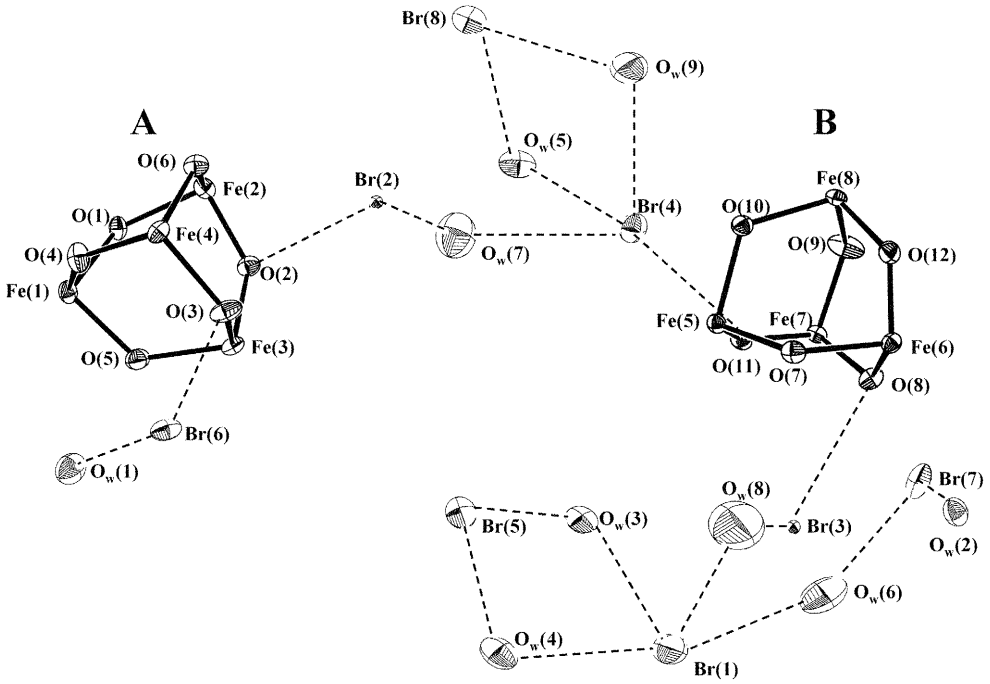

Figure 4. Structure of $[(tacn)_4Fe_4O_2(OH)_4]_2 \cdot 8Br \cdot 9H_2O$ showing 40% probability ellipsoids and atom labeling scheme. The O–H···Br hydrogen bonds (dashed lines) between Fe4 cations. For clarity, tacn ligands are omitted.

complex.

The X-ray analysis revealed that $[(tacn)_4Fe_4O_2(OH)_4]_2 \cdot 8Br \cdot 9H_2O$ involves two types of tetranuclear iron(III) cation complexes. Two Fe4 clusters show similar structures of adamantane skeletons but have different Fe···Fe distances. One having larger variation of Fe···Fe distances is labeled as *B*, and the other as *A*. In Figure 3, four Fe atoms of *A* are denoted as Fe(1), Fe(2), Fe(3) and Fe(4) and *B* as Fe(5), Fe(6), Fe(7) and Fe(8). As far as we know, the packing of two different Fe4 clusters is the first example though other adamantane-shaped tetranuclear metal complexes have been reported previously.[18-22] In the previous section, we discussed Fe–O lengths and Fe–O–Fe angles for only *A*. *B* has Fe-O(hydroxo) bond lengths and Fe–O(oxo) bond lengths of average 2.009 Å (1.992-2.027 Å) and average 1.806 Å (1.792-1.815 Å), respectively. Fe–O(hydroxo)–Fe angles and Fe–O(oxo) –Fe angles of average 123.6° (121.1-124.9°) and 132.3° (132.0-132.5°) for *B* are close to the values for *A*. Compared with *A*, *B* has shorter Fe–O(oxo) and longer Fe–O (hydroxo) bond lengths, which results in larger variation of Fe···Fe distances of *B*.

In the crystal structure, two kinds of Fe4 cations, *A* and *B*, which lie in general positions produce their enantiomers, *A'* and *B'* by the symmetry operations, four Fe4 cations in the crystal (Figure 3). *A'* is an enantiomer of *A* and *B'* is of *B* with respect of the same set of Fe···Fe distances but incapable to overlap between two enantiomers. The previous adamantane-shaped tetranuclear metal complexes also revealed to have racemic mixtures, though the existence of stereoisomers has not discussed in detail.[18(a),19-22]

As shown in Figure 4, *A* connects with *B* by the O–H···Br hydrogen bonds, represented as dashed lines, between the hydroxo ligands of *A* and *B*, a water molecule and two Br ions. *A* has a hydrogen bond tail connected with O(3) hydroxo ligand, and *B* also has a longer hydrogen bond tail of O(8) hydroxo ligand. The O–H···Br hydrogen bonds have average O···Br^- distance of 3.401 Å, a typical value for this type of hydrogen bond.[23] Figure 5 shows crystal packing of four kinds of Fe4 cations and supramolecular arrangement held together by the O–H···Br hydrogen bonds (solid and dashed lines) of average O···Br distance of 3.401 Å. For simplicity, bromide ions, and water molecules are omitted and hydrogen bonds are revealed to simple straight lines. In the unit cell, there are eight Fe4 cations, each pair of *A*, *A'*, *B* and *B'* cations. For helping the understanding of the connection between Fe4 clusters by the hydrogen bonds, Fe4s beyond the unit cell are shown in Figure 5. *A* and *A'* are located in almost (010) plane and *B* and *B'* in almost (020) plane. *B* cations along the *c*-axis are connected with each

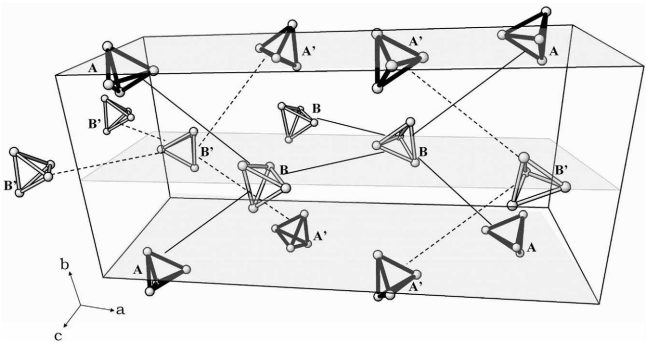

Figure 5. Packing structure of four types Fe4 clusters and supramolecular linkage by the O–H···Br hydrogen bonds (solid and dashed lines).

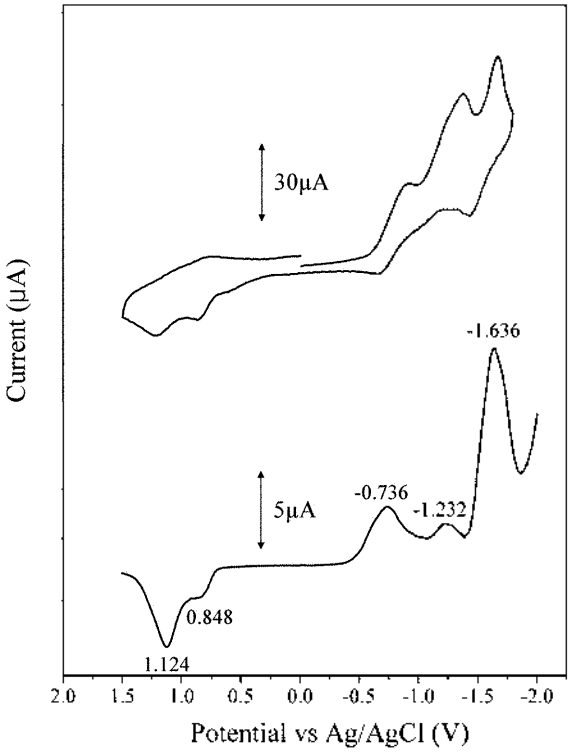

Figure 6. Cyclic voltammogram of Fe4 (1 mM) at 100 mV/s scan rate and its differential pulse voltammogram at 2 mV/s scan rate in methylene chloride containing 0.1 M $TBAPF_6$ (pulse amplitude 50 mV)

other forming 1D zigzag chains and each *B* is linked with near two *A* cations located in top and bottom, resulting in 3D supramolecular linkage. Connection between *B* cations are formed by the hydrogen bond of O(12) hydroxo of *B* and $O_W(2)$ water molecule located in the end of the hydrogen bond tail of another *B* (Figure 4). In addition to linkage between *B* and *A* by the hydrogen bond from O(2) to O(11) hydroxo ligands, *B* is linked with another *A* by the hydrogen bond between $O_W(9)$ and $O_W(1)$ of the hydrogen bond tail of *A*. Likewise *B*' are linked with another *B*' along the *c*-axis forming an 1D zigzag chain and with near two *A*' cations located in the upper and lower. In other words, hydrogen bonding network consisting of *A*' cations and *B*' cations has the same architecture of the linkage of *A* and *B* ones.

Electrochemistry. The electrochemical behavior of Fe4 has been studied using cyclic voltammetry (CV) and differential pulse voltammetry (DPV) in methylene chloride containing 0.1 M $TBAPF_6$ as supporting electrolyte, which are shown in Figure 6. There are three redox couples on the reduction side corresponding to the $Fe(III)_4/Fe(III)_3Fe(II)$, $Fe(III)_3Fe(II)/Fe(III)_2Fe(II)_2$ and $Fe(III)_2Fe(II)_2/Fe(III)Fe(II)_3$ forms of the complex at E_p = –0.736 V, –1.232 V and –1.636 V *vs* Ag/AgCl, respectively. two redox couples on the oxidation side corresponding to $Fe(III)_4/Fe(III)_3Fe(IV)$ and $Fe(III)_3Fe(IV)$ /$Fe(III)_2Fe(IV)_2$ forms reveal at E_p = 0.848 V and 1.124 V *vs* Ag/AgCl, respectively. These all redox couples are irreversible because the peak separation for each couple is much larger than E_p = 0.0592 V in the case of the reversible one and the DPV scans show broad and asymmetric peaks in contrast to the shaped and symmetric peak in the case of the reversible couple. Despite irreversible redox behavior, this complex is considerably stable for the redox process compared with other tetranuclear iron(III) clusters since three reductions and two oxidations of Fe4 are possible contrast to other tetranuclear iron(III) complex[24] which reveals only two redox couples at –0.5 V and –0.635 V *vs* Ag/AgCl.

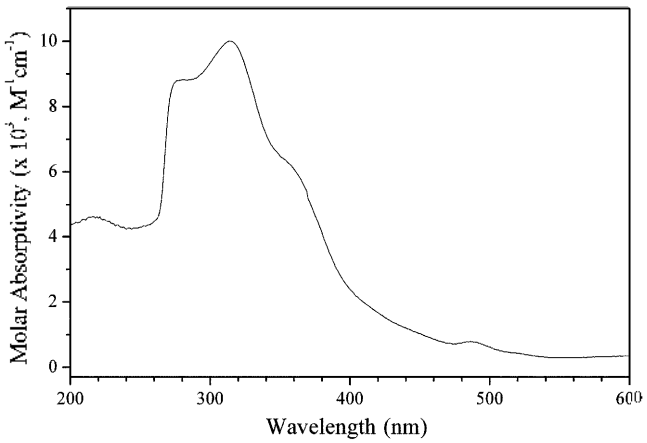

Figure 7. Electronic absorption spectrum of Fe4 in methylene chloride at 298 K.

Electronic Spectra. The electronic absorption spectrum of Fe4 is illustrated in Figure 7. All of the features observed in the UV/vis range are typical of the iron-oxo core. The transitions at 357 nm (ε = 6,080 $M^{-1}cm^{-1}$) and 486 nm (ε = 780 $M^{-1}cm^{-1}$) assigned as ligand-to-metal charge transfer (LMCT) bands are connected with the bridging oxide.[25] Intense transitions observed at 276 nm (ε = 8,800 $M^{-1}cm^{-1}$) and 314 nm (ε = 10,010 $M^{-1}cm^{-1}$) come from amine-to-iron(III) charge transfer (CT) bands.[26] The $n \rightarrow \sigma^*$ transitions at 216 nm (ε = 4,620 $M^{-1}cm^{-1}$) are also shown.

Magnetic Properties. Effective magnetic moment as a function of temperature is shown in Figure 8. The effective magnetic moment of the Fe4 at T = 350 K, μ_{eff} = 2.0 μ_B per Fe(III) ion, is smaller than 5.92 μ_B, the value for an uncorrelated Fe(III) ion spin with s = 5/2 and g = 2. The μ_{eff} decreases on lowering temperature and reaches a plateau around 50 K before dropping toward zero at lower temperature. In overall, the magnetic property is typical for an antiferromagnetically coupled system and similar to the behavior of the Wieghardt's complex, $[(tacn)_4Fe_4O_2(OH)_4]$-$I_4 \cdot 3H_2O$ [19] whose data fitting gave the exchange coupling constants of J = –106.3 (2) cm^{-1}, and J' = –15.1 (2) cm^{-1}, where J represents the exchange coupling *via* the oxo bridges and J' *via* the hydroxo bridges. In case of binuclear oxo- and hydroxo-bridged high spin Fe(III) complexes the exchange coupling via the oxo bridges is also stronger than that via the hydroxo bridges.[27] Since the present Fe4 and the Wieghardt's complex reveal similar tetranuclear skeletons and the similar Fe···Fe distances, Fe4 is expected to have the exchange coupling constants close to those for Wieghardt's complex. However, it is noted that Fe4 contains two types of

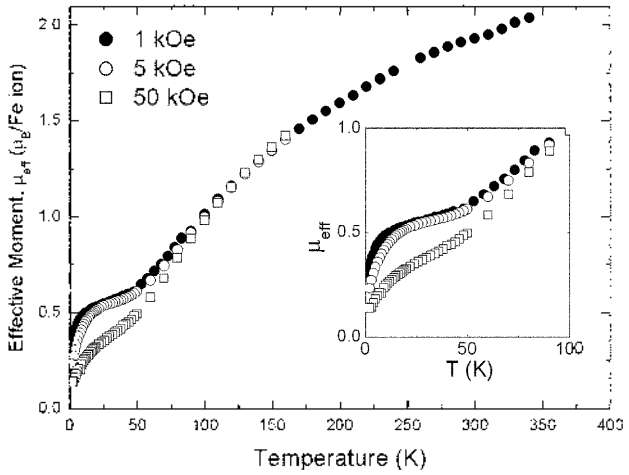

Figure 8. Temperature dependence of effective magnetic moment of μ_{eff} per Fe(III) ion spin.

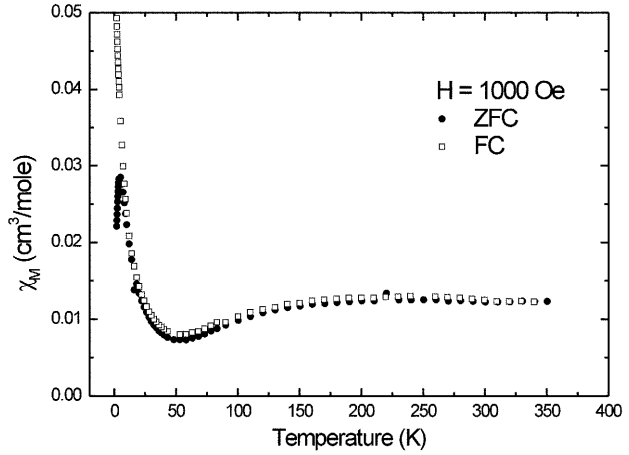

Figure 9. Molar magnetic susceptibility of $[(tacn)_4Fe_4O_2(OH)_4]_2$·8Br·9$H_2O$ *vs* temperature at H = 1 kOe, in zero field cooled (●) and field cooled (□).

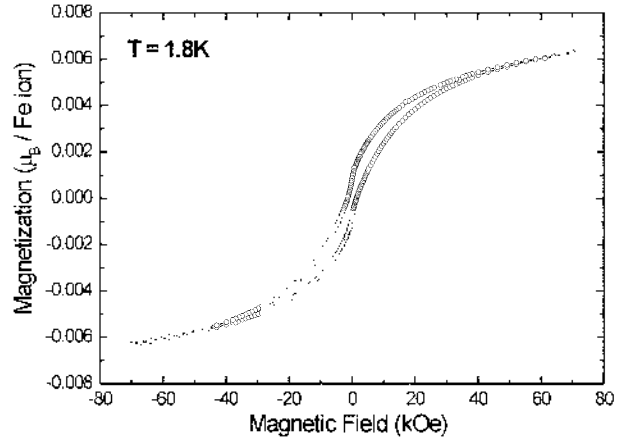

Figure 10. Magnetization per Fe(III) ion spin in Bohr magnetons vs applied magnetic field at T = 1.8 K.

tetranuclear moieties in the solid state, compared to the Wieghardt's complex with only one type, resulting in two sets of coupling constant values.

On the other hand, even for the strong AF coupling, the observation of the plateau in μ_{eff}(T) and its field dependence at low temperatures clearly indicates that there exist low-lying magnetic states. Although the origin of the low-lying magnetic states is not clearly understood at the moment,[22] their existence is clearly evident from the experimental data measured at low magnetic field (see the inset of Fig. 8).

As shown in Figure 9, despite antiferromagnetic coupling behavior of field cooled (FC) magnetic susceptibility, the zero field cooled (ZFC) data deviates from the FC data below approximately 14 K. The so-called blocking behavior implies that the low-lying magnetic states are slowly relaxing. The hysteresis behavior of magnetization at T = 1.8 K (Fig. 10), typical characteristic of slowly relaxing magnetic states, is also ascribed to the remnant magnetic moment due to the low-lying states.

Conclusion

A new tetranuclear iron(III) complex, Fe4, with iron-oxo core was successfully synthesized as single crystals. For the first time of adamantane-shaped tetranuclear metal complexes, two tetranuclear iron complexes showing the different Fe···Fe distances are packing in the crystal structure and form supramolecular arrangement by the hydrogen bonds. The overall magnetic properties are characterized by antiferromagnetic intramolecule interactions. From a careful measurement of magnetization at low magnetic fields and its field dependence, we observed a clear evidence of the low-lying, slowly relaxing magnetic states.

Acknowledgment. This work was supported by Electron Spin Science Center at POSTECH, which was established by the KOSEF.

Supporting Information Available: Crystallographic data for the structure reported here have been deposited with the Cambridge Crystallographic Data Centre (Deposition No. CCDC-258000). That data can be obtained free of charge *via* http://www.ccdc.cam.ac.uk/perl/catreq.cgi (or from the CCDC, 12 Union Road, Cambridge CB2 1EZ, UK; fax: +44 1223 336033; e-mail: deposit@ccdc.cam.ac.uk). The file, in CIF format, for $[(tacn)_4Fe_4O_2(OH)_4]_2$·8Br·9$H_2O$ will be also given upon your request to the corresponding author.

References

1. (a) Awschalom, D. D.; Di Vincenzo, D. P.; Smyth, J. F. *Physics Today* **1995**, *48*, 43. (b) Stamp, P. C. E. *Nature* **1996**, *383*, 125. (c) Thomas, L.; Lionti, F.; Ballou, R.; Gatteschi, D.; Sessoli, R.; Barabara, B. *Nature* **1996**, *383*, 145.
2. (a) Gatteschi, D.; Caneschi, A.; Pardi, L.; Sesoli, R. *Science* **1994**, *265*, 1054. (b) Murray, K. S. *Adv. Inorg. Chem.* **1995**, *43*, 261. (c) Eppley, H. J.; Tsai, H. L.; Folting, K.; Christou, G; Hendrickson, D. N. *J. Am. Chem. Soc.* **1995**, *117*, 301.
3. (a) Caneschi, A.; Gatteschi, D.; Sesoli, R. *J. Chem. Soc., Dalton Trans.* **1997**, 3963. (b) Solomon, E. I.; Sundaram, U. M.; Machonkin, T. E. *Chem. Rev.* **1996**, *96*, 2563. (c) Dismukes, G. C.

Chem. Rev. **1996**, *96*, 2909. (d) Law, N. A.; Caudle, M. T.; Pecoraro, V. L. *Adv. Inorg. Chem.* **1998**, *46*, 305.
4. (a) Lippard, S. J. *Angew. Chem., Int. Ed. Engl.* **1988**, *27*, 344. (b) Kurtz, J. D. M. *Chem. Rev.* **1990**, *90*, 585. (c) Feig, A. L.; Lippard, S. J. *Chem. Rev.* **1994**, *94*, 759. (d) Wilkins, R. G.; Harrington, P. C. *Adv. Inorg. Biochem.* **1983**, *5*, 51. (e) Sjoberg, B.; Graslund, A. *Ibid.* **1983**, *5*, 87. (f) Antanaitis, B. C.; Aisen, P. *Ibid.* **1983**, *5*, 111.
5. (a) Clegg, G. A.; Fiitton, J. E.; Harrison, P. M.; Treffry, A. *Prog. Biophys. Mol. Biol.* **1980**, *36*, 53. (b) Tow, K. *J. Biol. Chem.* **1982**, *256*, 9377. (c) Thiel, E. C.; Sayers, D. E.; Brown, M. A. *J. Biol. Chem.* **1979**, *254*, 8132. (d) Spiro, T. G.; Pope, L.; Saltman, P. *J. Am. Chem. Soc.* **1967**, *89*, 5555. (e) Spiro, T. G.; Bates, G.; Saltman, P. *J. Am. Chem. Soc.* **1967**, *89*, 5559. (f) Theil, E. C. *Adv. Inorg. Biochem.* **1983**, *5*, 1. (g) Fischbach, F. A.; Anderegg, J. W. *J. Mol. Biol.* **1965**, *14*, 458. (h) Smith, J. M. A.; Helliwell, J. R. *Inorg. Chim. Acta* **1985**, *106*, 193. (i) Mann, S.; Bannister, J. V.; Williams, R. J. P. *J. Mol. Biol.* **1986**, *188*, 225.
6. (a) Sydora, O. L.; Wolczanski, P. T.; Lobkovsky, E. B. *Angew. Chem., Int. Ed.* **2003**, *42*, 2685. (b) Caneschi, A.; Cornia, A.; Fabretti, A. C.; Gatteschi, D. *Angew. Chem., Int. Ed.* **1999**, *38*, 1295. (c) Zhou, H.; Holm, R. H. *Inorg. Chem.* **2003**, *42*, 11. (d) You, J.; Snyder, B. S.; Papaefthymiou, G. C.; Holm, R. H. *J. Am. Chem. Soc.* **1990**, *112*, 1067.
7. (a) Sessoli, R.; Gatteschi, D. *Angew. Chem., Int. Ed.* **2003**, *42*, 268. (b) Aromi, G.; Aubin, S. M. J.; Bolcar, D. N.; Huffman, J. C.; Squire, R. C.; Tsai, H. L.; Wang, S.; Wemple, M. W. *Polyhedron* **1998**, *17*, 3005. (c) Awschalom, D. D.; Di Vincenzo, D. P.; Smyth, J. F. *Science* **1992**, *258*, 414. (d) Barbara, B.; Sampaio, L. C.; Wegrowe, J. E.; Ratnam, B. A.; Marchand, A.; Paulsen, C.; Novak, M. A.; Tholence, J. L.; Uehara, M.; Fruchart, D. *J. Appl. Phys.* **1993**, *73*, 6703. (e) Tejada, J.; Ziolo, R. F.; Zhang, X. X. *Chem. Mater.* **1996**, *8*, 1784. (f) Caneschi, A.; Ohm, T.; Paulsen, C.; Rovai, D.; Sangregorio, C.; Sessoli, R. *J. Magn. Magn. Mater.* **1998**, *177*, 1330.
8. (a) Wernsdorfer, W.; Sessoli, R.; Caneschi, A.; Gatteschi, D.; Cornia, A.; Mailly, D. *J. Appl. Phys.* **2001**, *87*, 5481. (b) Wernsdorfer, W.; Caneschi, A.; Sessoli, R.; Gatteschi, D.; Cornia, A.; Villar, V.; Paulsen, C. *Phys. Rev. Lett.* **2000**, *84*, 2965. (c) Furukawa, Y.; Watanabe, K.; Kumagai, K.; Jang, Z.; Lascialfari, A.; Borsa, F.; Gatteschi, D. *Phys. Rev. B* **2000**, *62*, 14246. (d) Lascialfari, A.; Jang, Z.; Borsa, F.; Carretta, P.; Gatteschi, D. *Phys. Rev. Lett.* **1998**, *81*, 3773.
9. Barra, A. L.; Caneschi, A.; Cornia, A.; Fabrizi de Biani, F.; Gatteschi, D.; Sangregorio, C.; Sessoli, R.; Sorace, L. *J. Am. Chem. Soc.* **1999**, *121*, 5302.
10. (a) Lis, T. *Acta Cryst.* **1980**, *B36*, 2042. (b) Sessoli, R.; Gatteschi, D.; Caneschi, A.; Novak, M. A. *Nature* **1993**, *365*, 141. (c) Thomas, L.; Lionti, F.; Ballou, R.; Gatteschi, D. *Nature* **1996**, *383*, 145. (d) Chudnovsky, E. M. *Science* **1996**, *274*, 938. (e) Friedman, J. R.; Sarachik, M. P. *Phy. Rev. Lett.* **1996**, *76*, 3830. (f) Jeon, W. S.; Jin, M. K.; Kim, Y. J.; Jung, D. Y.; Suh, B. J.; Yoon, S. W. *Bull. Korean Chem. Soc.* **2004**, *25*, 1036.
11. (a) Wernsdorfer, W.; Allaga-Alcalde, N.; Hendrickson, D. N.; Christou, G. *Nature* **2002**, *416*, 406. (b) Aubin, S. M. J.; Wemple, M. W.; Adams, D. M.; Tsai, H.; Christou, G.; Hendrickson, D. N. *J. Am. Chem. Soc.* **1996**, *118*, 7746.
12. Wieghardt, K.; Pohl, K.; Jibril, I.; Huttner, G. *Angew. Chem., Int. Ed.* **1984**, *23*, 77.
13. (a) Armstrong, W. H.; Roth, M. E.; Lippard, S. J. *J. Am. Chem. Soc.* **1987**, *109*, 6318. (b) Jameson, D. L.; Xie, C. L.; Hendrickson, D. N.; Potenza, J. A.; Schugar, H. L. *J. Am. Chem. Soc.* **1987**, *109*, 740. (c) Moore, P. B. *Am. Mineral.* **1972**, *57*, 397. (d) Miyasato, Y.; Nogami, Y.; Ohba, M.; Sakiyama, H.; Okawa, H. *Bull. Chem. Soc. Jpn.* **2003**, *76*, 1009.
14. Wieghardt, K.; Pohl, K.; Gebert, W. *Angew. Chem., Int. Ed.* **1983**, *22*, 727.
15. (a) *SMART*, version 5.0; data collection software; Bruker AXS, Inc.; Madison, WI, 1998. (b) *SAINT*, version 5.0; data intergration software; Bruker AXS, Inc.; Madison, WI, 1998.
16. *Sheldrick*, G. M. *SADABS, A Program for Absorption Correction with the Bruker SMART System*; Universitat Göttingen; Göttingen, Germany, 1996.
17. McArdle, P. *SHELX-86 and SHELX-97 Users Guide*; Crystallography Center, Chemistry Department, National University of Ireland; Galway, Ireland; *J. Appl. Crystallogr.* **1995**, *28*, 65.
18. (a) Murch, B. P.; Boyle, P. D.; Que, L. *J. Am. Chem. Soc.* **1985**, *107*, 6728. (b) Zhang, L.; Yan, S.; Li, C.; Liao, D.; Jiang, Z.; Cheng, P.; Wang, G.; Weng, L.; Leng, X. *J. Chem. Crystallogr.* **2000**, *30*, 251. (c) Wieghardt, K.; Bossek, U.; Gebert, W. *Angew. Chem., Int. Ed.* **1983**, *22*, 328. (d) Murch, B. P.; Bradley, F. C.; Boyle, P. D.; Papaefthymiou, V.; Que, L., Jr. *J. Am. Chem. Soc.* **1987**, *109*, 7993.
19. Drueke, S.; Wieghardt, K.; Nuber, B.; Weiss, J.; Bominaar, E. L.; Sawaryn, A.; Winkler, H.; Trautwein, A. X. *Inorg. Chem.* **1989**, *28*, 4477.
20. Dube, C. E.; Wright, D. W.; Pal, S.; Bonitatebus, P. J.; Armstrong, W. H. *J. Am. Chem. Soc.* **1998**, *120*, 3704.
21. Wieghardt, K.; Bossek, U.; Nuber, B.; Weiss, J.; Bonvoisin, J.; Corbella, M.; Vitols, S. E.; Girerd, J.-J. *J. Am. Chem. Soc.* **1988**, *110*, 7398.
22. Zipse, D.; Abboud, K. A.; Dalal, N. S. *J. Appl. Phys.* **2003**, *93*, 7086. The atomic coordinates are not included in the paper and we referred to the file No. of 238761 from the CCDC.
23. (a) Braga, D.; Grepioni, F.; Orpen, A. G. *Crystal Engineering: From Molecules and Crystals to Materials*; Kluwer Academic Publishers; Dordrecht, 1999; Chapter 6. (b) Ahn, D. S.; Jeon, I. S.; Jang, S. H.; Park, S. W.; Lee, S.; Cheong, W. *Bull. Korean Chem. Soc.* **2003**, *24*, 695.
24. Sessler, J. L.; Sibert, J. W.; Lynch, V. *Inorg. Chem.* **1993**, *32*, 621.
25. Brown, C.; Remar, G.; Musselman, R.; Solomon, E. *Inorg. Chem.* **1995**, *34*, 688.
26. Snodin, M. D.; Ould-Moussa, L.; Wallmann, U.; Lecomte, S.; Bachler, V.; Bill, E.; Hummel, H.; Weyhermuller, T.; Hildebrandt, P.; Wieghardt, K. *Chem. Eur. J.* **1999**, *5*, 2554.
27. Gorun, S. M.; Lippard, S. J. *Inorg. Chem.* **1991**, *30*, 1625.